 Open access • Posted Content • DOI:10.1101/590380

A Membrane-Bound Cytochrome Enables Methanosarcina acetivorans to Conserve Energy to Support Growth from Extracellular Electron Transfer — [Source link](#)

Dawn E. Holmes, Dawn E. Holmes, Toshiyuki Ueki, Hai-Yan Tang ...+7 more authors

Institutions: Western New England University, University of Massachusetts Amherst, Nanjing Agricultural University, Dalian University of Technology ...+1 more institutions

Published on: 26 Mar 2019 - bioRxiv (Cold Spring Harbor Laboratory)

Topics: Methanosarcina acetivorans, Methanosarcina, Methanogen, Geobacter and Electron acceptor

Related papers:

- [A Membrane-Bound Cytochrome Enables Methanosarcina acetivorans To Conserve Energy from Extracellular Electron Transfer.](#)
- [Physiological Evidence for Isopotential Tunneling in the Electron Transport Chain of Methane-Producing Archaea.](#)
- [Anaerobic growth of Methanosarcina acetivorans C2A on carbon monoxide: An unusual way of life for a methanogenic archaeon](#)
- [Rerouting Cellular Electron Flux To Increase the Rate of Biological Methane Production](#)
- [Extracellular Electron Uptake by Two Methanosarcina Species](#)

Share this paper:    

View more about this paper here: <https://typeset.io/papers/a-membrane-bound-cytochrome-enables-methanosarcina-3da86vqd7l>

1 A Membrane-Bound Cytochrome Enables *Methanosarcina acetivorans* to Conserve
2 Energy to Support Growth from Extracellular Electron Transfer

3

4 Dawn E Holmes*^{1,2}, Toshiyuki Ueki*¹, Hai-Yan Tang^{1,3}, Jinjie Zhou^{1,4}, Jessica A
5 Smith^{1,5}, Gina Chaput¹, and Derek R Lovley¹

6

7 ¹Department of Microbiology, University of Massachusetts Amherst, Morrill IV N
8 Science Center, Amherst, MA 01003, USA

9 ²Department of Physical and Biological Sciences, Western New England University,
10 Springfield, MA, 01119, USA

11 ³Jiangsu Provincial Key Lab for Organic Solid Waste Utilization, National Engineering
12 Research Center for Organic-based Fertilizers, Jiangsu Collaborative Innovation
13 Center for Solid Organic Waster Resource Utilization, Nanjing Agricultural
14 University, Nanjing, 210095, China

15 ⁴School of Life Science and Biotechnology, Dalian University of Technology, Dalian,
16 Liaoning Province, China, 116024

17 ⁵Department of Biology, American International College, Springfield, MA

18 *Both authors contributed equally

19 Keywords: anaerobic respiration, extracellular electron transfer, anthraquinone-2,6,-
20 disulfonate reduction, AQDS reduction, Rnf complex, *c*-type cytochrome,
21 methanogen, archaea

22 Running title: Cytochrome facilitates AQDS reduction by methanogen

23 **Abstract**

24 Conservation of energy to support growth solely from extracellular electron transfer was
25 demonstrated for the first time in a methanogen. *Methanosarcina acetivorans* grew with
26 methanol as the sole electron donor and the extracellular electron acceptor anthraquinone-
27 2,6-disulfonate (AQDS) as the sole electron acceptor when methane production was
28 inhibited with bromoethanesulfonate. Transcriptomics revealed that transcripts for the
29 gene for the transmembrane, multi-heme, *c*-type cytochrome MmcA were 4-fold higher
30 in AQDS-respiring cells versus methanogenic cells. A strain in which the gene for MmcA
31 was deleted failed to grow via AQDS reduction whereas strains in which other
32 cytochrome genes were deleted grew as well as the wild-type strain. The MmcA-deficient
33 strain grew with the conversion of methanol or acetate to methane, suggesting that
34 MmcA has a specialized role as a conduit for extracellular electron transfer. Enhanced
35 expression of genes for methanol conversion to methyl-coenzyme M and components of
36 the Rnf complex suggested that methanol is oxidized to carbon dioxide in AQDS-
37 respiring cells through a pathway that is similar to methyl-coenzyme M oxidation in
38 methanogenic cells. However, during AQDS respiration the Rnf complex and reduced
39 methanophenazine probably transfer electrons to MmcA, which functions as the terminal
40 reductase for AQDS reduction. Extracellular electron transfer may enable survival of
41 methanogens in dynamic environments in which oxidized humic substances and Fe(III)
42 oxides are intermittently available. The availability of tools for genetic manipulation of
43 *M. acetivorans* makes it an excellent model microbe for evaluating *c*-type cytochrome-
44 dependent extracellular electron transfer in Archaea.

45

46 **Importance**

47 Extracellular electron exchange in *Methanosarcina* species and closely related Archaea
48 plays an important role in the global carbon cycle and can enhance the speed and stability
49 of anaerobic digestion, an important bioenergy strategy. The potential importance of
50 *c*-type cytochromes for extracellular electron transfer to syntrophic bacterial partners
51 and/or Fe(III) minerals in some Archaea has been suspected for some time, but the
52 studies with *Methanosarcina acetivorans* reported here provide the first genetic evidence
53 supporting this hypothesis. The results suggest parallels with Gram-negative bacteria,
54 such as *Shewanella* and *Geobacter* species, in which outer-surface *c*-type cytochromes
55 are an essential component for electrical communication with the extracellular
56 environment. *M. acetivorans* offers an unprecedented opportunity to study mechanisms
57 for energy conservation from the anaerobic oxidation of one-carbon organic compounds
58 coupled to extracellular electron transfer in Archaea with implications not only for
59 methanogens, but possibly also for anaerobic methane oxidation.

60 **Introduction**

61 Extracellular electron exchange is central to the environmental function of diverse
62 Archaea that oxidize and/or produce methane. Some methane-producing microorganisms
63 can divert electron transfer from methane production to the reduction of extracellular
64 electron carriers such as Fe(III), U(VI), V(IV), and anthraquinone-2,6-disulfonate
65 (AQDS), a humic acid analog (1-9). Diversion of electron flux from methane production
66 to extracellular electron transfer may influence the extent of methane production and
67 metal geochemistry in anaerobic soils and sediments. Methanogens such as *Methanotherix*
68 (formerly *Methanosaeta*) and *Methanosarcina* species can accept electrons via direct
69 interspecies electron transfer from electron-donating partners, such as *Geobacter* species

70 in important methanogenic environments such as anaerobic digesters and rice paddy soils
71 (10-12). Anaerobic methane oxidation also plays an important role in the global carbon
72 cycle and diverse anaerobic methane-oxidizing archaea (ANME) transfer electrons
73 derived from methane oxidation to extracellular electron acceptors, such as other
74 microbial species, Fe(III), or extracellular quinones (13-19). The electrical contacts for
75 extracellular electron exchange have yet to be definitively identified in any of these
76 Archaea.

77 It has been hypothesized that outer-surface cytochromes enable electron transfer
78 to electron-accepting microbial partners or Fe(III) in some ANME (13-19). Genes for
79 multi-heme *c*-type cytochromes that are present in ANME genomes can be highly
80 expressed and in some instances the proteins have been detected. The putative function of
81 outer-surface cytochromes is terminal electron transfer to extracellular electron acceptors,
82 similar to the role that outer surface *c*-type cytochromes play in extracellular electron
83 transfer in Gram-negative bacteria such as *Shewanella* and *Geobacter* species (20-22).
84 Similar *c*-type cytochrome electrical contacts have been proposed for Fe(III)-reducing
85 Archaea such as *Ferroglobus* and *Geoglobus* species (23, 24). However, the study of the
86 mechanisms for extracellular electron transfer in these archaea has been stymied by the
87 lack of microorganisms available in pure culture that can grow via extracellular electron
88 transfer and are genetically tractable.

89 Tools are available for genetic manipulation of the methanogen *Methanosarcina*
90 *acetivorans* (25-27). A methyl-coenzyme M reductase from an uncultured ANME was
91 introduced into *M. acetivorans* to generate a strain that could convert methane to acetate
92 with simultaneous reduction of Fe(III) (28). Most of the electrons from the methane

93 consumed were recovered in acetate (28) and it was not shown that energy was conserved
94 from Fe(III) reduction. *In vitro* reactions catalyzed by membrane vesicles of wild-type *M.*
95 *acetivorans* suggested that the membrane-bound heterodisulfide reductase HdrDE
96 reduced Fe(III)-citrate and AQDS, and that an outer-surface multi-heme *c*-type
97 cytochrome, might also function as a potential electron donor for Fe(III)-citrate reduction
98 (29). However, *in vitro* assays with cell components are not a definitive approach for
99 determining the physiologically relevant mechanisms involved in the reduction of Fe(III)
100 and AQDS because many reduced co-factors and redox-proteins, including *c*-type
101 cytochromes, can non-specifically reduce these electron acceptors (30). Analysis of the
102 phenotypes of intact cells that result from specific gene deletions can provide more
103 conclusive evidence.

104 Here we report that *M. acetivorans* can be grown in the absence of methane
105 production with AQDS as the sole electron acceptor. Analysis of gene expression
106 patterns and phenotypes of gene deletion strains suggest a mechanism for energy
107 conservation during extracellular electron transfer.

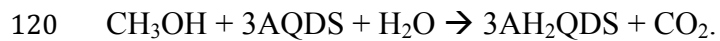
108

109 **Results and Discussion**

110 **Growth of *M. acetivorans* with AQDS as the sole terminal electron acceptor**

111 In medium with methanol provided as the electron donor and AQDS as a potential
112 electron acceptor, *M. acetivorans* simultaneously produced methane and reduced AQDS
113 (Figure 1a). The addition of bromoethanesulfonate (BES) inhibited methane production
114 and increased the extent of AQDS reduction (Figure 1b; Supplementary Figure S1).
115 Metabolism of methanol (Figure 1c) was accompanied by cell growth (Figure 1d). In the

116 BES-amended cultures 6.2 mM methanol was consumed with the reduction of 15.7 mM
117 AQDS. When the need to divert some of the methanol metabolized to cell biomass is
118 considered, this stoichiometry is consistent with the oxidation of methanol to carbon
119 dioxide with AQDS serving as the sole electron acceptor:



121 The greater consumption of methanol in the absence of BES (Figure 1c), was in
122 accordance with the extent of AQDS reduction and the simultaneous conversion of
123 methanol to methane: $4\text{CH}_3\text{OH} \rightarrow 3\text{CH}_4 + \text{CO}_2 + 2\text{H}_2\text{O}$.

124 The methanol oxidation coupled with AQDS reduction in the presence of BES
125 described here is the first demonstration of a methanogen conserving energy to support
126 growth with electron transfer to an external electron acceptor as the sole means of energy
127 conservation. The ability of *M. acetivorans* to grow in this manner, and the availability of
128 tools for genetic manipulation (25-27) provide the opportunity for functional analysis of
129 extracellular electron transfer in an archaeon.

130 **Transcriptomics and gene deletion studies demonstrate that the multi-heme *c*-type** 131 **cytochrome Mmca is important for AQDS reduction**

132 In order to obtain insight into potential electron carriers involved in AQDS
133 reduction, the transcriptome of cells grown with AQDS as the sole electron acceptor in
134 the presence of BES was compared with the transcriptome of cells grown with methanol
135 in the absence of AQDS or BES, so that methane production was the sole route of
136 electron flux. The median \log_2 RPKM value for the cells grown via methanogenesis (5.2)
137 was substantially higher than for the cells grown via AQDS reduction (4.0). These results
138 are consistent with the finding that cells grown via methanogenesis grew ~4 times faster

139 than cells respiring AQDS (generation time for AQDS-respiring cells was 3 days vs 0.7
140 days for methanogenic cells).

141 Remarkably, despite the overall lower transcription rate of cells grown via AQDS
142 reduction, the transcripts for gene MA0658, which encodes a seven-heme, outer-surface
143 *c*-type cytochrome, were 4-fold higher in AQDS-reducing versus methanogenic cells
144 (Table 1, Supplementary Table S1A). For future reference, this cytochrome was
145 designated MmcA (membrane multi-heme cytochrome A). Multi-heme *c*-type
146 cytochromes are of particular interest as potential electron carriers in extracellular
147 electron transport because of the well-documented role of multi-heme *c*-type
148 cytochromes in bacteria such as *Shewanella* and *Geobacter* species that are highly
149 effective in extracellular electron transfer (20-22). MA3739, a gene coding for a five-
150 heme *c*-type cytochrome, was transcribed at similar levels as *mmcA*, and 4 fold more
151 transcripts were detected in AQDS-reducing than methanogenic cells (Table 1).

152 There are three other putative *c*-type cytochrome genes in the *M. acetivorans*
153 genome (31). Transcripts for MA0167, which encodes a mono-heme cytochrome with
154 predicted localization in the cell membrane, were 6-fold more abundant in cells grown
155 via AQDS respiration (Table 1). Functional analysis of the outer-membrane of *G.*
156 *sulfurreducens* has suggested that a mono-heme *c*-type cytochrome may play a role in
157 regulating the expression of multi-heme *c*-type cytochromes, possibly by providing a
158 sensor function (32, 33). It is possible that the protein encoded by MA0167 is playing a
159 similar role in *M. acetivorans*. The number of transcripts for MA2925 and MA2908, both
160 of which encode two-heme *c*-type cytochromes, was comparable in AQDS-reducing
161 versus methanogenic cells (Table 1). These cytochromes are homologous to methylamine

162 utilization protein G (MauG) and di-heme cytochrome c peroxidase (CcpA). MauG is
163 required for aerobic methylamine metabolism (34-36), and CcpA proteins reduce
164 hydrogen peroxide to water and protect the cell from reactive oxygen species (37, 38).
165 Thus, it seems unlikely that either of these cytochromes is involved in extracellular
166 electron transfer.

167 In order to evaluate the potential role of *c*-type cytochromes in AQDS reduction,
168 deletion mutant strains were constructed in *M. acetivorans* for each *c*-type cytochrome
169 gene in the genome (Table 1). Only the deletion of *mmcA* inhibited AQDS reduction
170 (Figure 2a). Deletion of *mmcA* had a slight impact on methanogenic growth with
171 methanol (Figure 2b).

172 These results suggest that MmcA is an essential component for extracellular
173 electron transfer to AQDS, but not for the conversion of methanol to methane. This
174 conclusion was further supported by the finding that *mmcA* was highly transcribed in
175 AQDS-reducing cells, however, its expression levels were below the median log₂ RPKM
176 values for methanogenic cells (Table 1 and Supplementary Table S1).

177 Previous studies have suggested that MmcA is part of the Rnf complex, which is
178 required for acetoclastic methanogenesis (39) and that it is co-transcribed with Rnf genes
179 located in the same region of the chromosome (40). However, deletion of the MmcA
180 gene did not substantially impact growth on acetate (Figure 2B) or transcription of other
181 genes from the Rnf complex (Supplementary Figure S2). Furthermore, the expression
182 profiles of *mmcA* and genes for the Rnf complex were also different (Tables 1 and 2).

183 **Model for Electron Transport to AQDS via MmcA**

184 MmcA is a strong candidate for the terminal AQDS reductase because its
185 localization in the cell membrane (40) is likely to provide access to AQDS and because
186 of the well-known role of outer-membrane multi-heme *c*-type cytochromes in reduction
187 of AQDS and various forms of Fe(III) in Gram-negative bacteria such as *Shewanella* and
188 *Geobacter* species (20-22, 41). It was previously suggested that MmcA could be a
189 terminal reductase for the reduction of soluble Fe(III)-citrate, based on the *in vitro*
190 oxidation of MmcA in membrane vesicles upon addition of Fe(III)-citrate (29). Such *in*
191 *vitro* assays can be poor predictors of *in vivo* activity because Fe(III)-citrate typically
192 oxidizes *c*-type cytochromes *in vitro*, regardless of physiological function, due to its very
193 positive redox potential. However, as detailed below, multiple lines of evidence support a
194 model in which energy can be conserved when MmcA serves as the terminal reductase
195 during methanol oxidation coupled to AQDS reduction (Figure 3).

196 During methane production from methanol, methanol is converted to CH₃-CoM
197 by the activity of three enzymes, methyltransferase 1 (MtaB), methyltransferase 2
198 (MtaA), and methanol corrinoid protein (MtaC) (42-44). The oxidation of one molecule
199 of CH₃-CoM to CO₂ generates the reducing equivalents necessary to reduce three
200 molecules of CH₃-CoM to methane. During methanol oxidation coupled to AQDS
201 reduction in the presence of BES, the step that reduces CH₃-CoM to methane is blocked,
202 but the option for CH₃-CoM oxidation remains (Figure 3). Genes coding for enzymes
203 involved in the oxidation of CH₃-CoM to carbon dioxide were more highly expressed in
204 methanogenic cells, consistent with increased overall transcriptional activity in
205 methanogenic cells and the need for this pathway to generate reductants to support
206 methanogenesis (Supplementary Table S2). However, transcription of genes coding for

207 enzymes involved in CH₃-CoM oxidation were also well above the median log₂ RPKM
208 value in the AQDS-respiring cells, suggesting that this pathway is also important for
209 methanol oxidation coupled to AQDS reduction (Supplementary Tables S1A).

210 Differential expression of genes encoding isomers of MtaB, MtaA, and MtaC
211 suggested that there might be some differences in the route for methanol conversion to
212 CH₃-CoM (Table 3). The genes for the isomers MtaB1, MtaA1, and MtaC1 were more
213 highly expressed in methanogenic cells, whereas AQDS-respiring cells had higher
214 transcript abundance for genes coding for the alternative MtaB, MtaA, and MtaC isomers
215 (Table 3). Differences in the activity of these isomers are unknown, but in previous
216 studies *mtaA1*, *mtaB1*, and *mtaC1* genes were specifically transcribed during
217 methanogenesis from methanol and MtaA1 was required for growth on methanol,
218 whereas MtaA2 was dispensable (44).

219 Oxidation of methanol to carbon dioxide is expected to yield reduced ferredoxin
220 and reduced F₄₂₀ (F₄₂₀H₂). It is likely that the Rnf complex oxidizes reduced ferredoxin
221 with electron transfer to MmcA (45). Despite the lower overall gene transcript abundance
222 in AQDS-respiring cells, transcripts for genes coding for components of the Rnf complex
223 were slightly higher than those in methanogenic cells (Table 2), suggesting an important
224 role for the Rnf complex in energy conservation from methanol oxidation coupled to
225 AQDS reduction.

226 In methanogenic cells the membrane-bound Fpo complex (F₄₂₀:methanophenazine
227 oxidoreductase) oxidizes F₄₂₀H₂ derived from methanol oxidation with the reduction of
228 methanophenazine and proton extrusion (46-50). Transcript abundance for all Fpo
229 subunit genes was higher in methanogenic cells than AQDS-reducing cells, as expected

230 because of the importance of Fpo in oxidizing $F_{420}H_2$ in cells producing methane and the
231 overall higher gene expression levels in methanogenic cells (Supplementary Table S3).
232 However, the number of transcripts for all of the Fpo complex genes was significantly
233 higher than the median \log_2 RPKM value in AQDS-respiring cells (Supplementary Table
234 S1A), suggesting that Fpo is important for the oxidation of $F_{420}H_2$ generated in methanol-
235 oxidizing, AQDS-reducing cells. The reduced methanophenazine that Fpo generates from
236 $F_{420}H_2$ oxidation can transfer electrons to MmcA (39, 40, 45, 51). Although it has also
237 been proposed that reduced methanophenazine may be able to directly transfer electrons
238 to extracellular electron carriers in *M. acetivorans* (29), the requirement for MmcA for
239 growth via AQDS reduction indicates that this is an unlikely route for AQDS reduction.

240 In methanogenic cells, reduced methanophenazine can also donate electrons to the
241 membrane-bound heterodisulfide reductase HdrDE (50, 52-55). *In vitro* evidence with
242 membrane-vesicles suggested that HdrDE can reduce AQDS with CoM-SH and CoB-SH
243 oxidation to form CoM-S-S-CoB (29). However, the redox-active components of HdrDE
244 responsible for electron transfer to an electron acceptor are localized to the cytoplasmic
245 side of the membrane (50) and thus unlikely to access extracellular AQDS *in vivo*. The
246 relative expression of *hdrD* and *hdrE* was slightly lower in AQDS-reducing cells than
247 methanogenic cells (Supplementary Table S1). Furthermore, the inability of the MmcA-
248 deficient strain to grow via AQDS reduction indicates that HdrDE is not capable of
249 functioning as the sole AQDS reductase to support growth. Thus, in the lack of strong
250 evidence for a role for HdrDE, the likely simpler and more direct route for AQDS-
251 dependent oxidation of reduced methanophenazine is electron transfer to MmcA.

252 From these considerations, and the current understanding of the function of the
253 redox proteins involved (50, 56, 57), a positive balance of Na^+ and H^+ outside the cell to
254 support the generation of ATP during AQDS respiration is possible (Figure 3). In this
255 model two Na^+ must be translocated into the cell for the initial oxidation of $\text{CH}_3\text{-S-CoM}$.
256 Two moles of F_{420}H_2 and one mole of reduced ferredoxin are generated per mole of $\text{CH}_3\text{-}$
257 S-CoM oxidized to carbon dioxide. Fpo oxidizes the F_{420}H_2 with H^+ extrusion and the
258 reduction of methanophenazine. The reduced methanophenazine transfers electrons to
259 MmcA, which reduces AQDS. The Rnf complex oxidizes the reduced ferredoxin coupled
260 with Na^+ translocation and the reduction of MmcA. MmcA may transfer protons as well
261 as electrons during AQDS reduction as observed in other *c*-type cytochromes (58-63).
262 The ATP synthase couples both Na^+ and H^+ transport to ATP synthesis (64), but the
263 H^+/Na^+ antiporter complex Mrp can be important for balancing external Na^+/H^+ ratios
264 (65). Genes for Mrp were highly expressed in AQDS-reducing cells (Table 2).

265 Uncertainties in the stoichiometry of Na^+/H^+ transport per ATP synthesized and
266 the total amount of H^+ translocated prevent an accurate estimate of the theoretical ATP
267 yield per mole of methanol oxidized with the reduction of AQDS. However, it is clear
268 that net ATP synthesis is likely from the proposed metabolic route, consistent with the
269 observed growth of *M. acetivorans* with methanol oxidation coupled to AQDS reduction.

270

271 **Implications**

272 The discovery that *M. acetivorans* can conserve energy to support growth from
273 the oxidation of a one-carbon compound coupled to the reduction of an extracellular
274 electron acceptor has important implications for the biogeochemistry of anaerobic soils

275 and sediments and provides a genetically tractable model microbe for further analysis of
276 the mechanisms of extracellular electron transfer in *Archaea*. Humic substances and
277 Fe(III) are often abundant extracellular electron acceptors in a wide variety of anaerobic
278 soils and sediments and their availability for microbial respiration can reduce the extent
279 of methane production (66-69). Competition for electron donors between methanogens
280 and Fe(III)- and humics-reducing microorganisms is one factor (70, 71). However, the
281 finding that some methanogens may conserve energy by reducing extracellular electron
282 acceptors suggests a mechanism for methanogens to survive in environments in which
283 Fe(III) and oxidized forms of humic substances are abundant and then rapidly switch to
284 methane production as these extracellular electron acceptors are depleted.

285 A comprehensive survey of the ability of diverse methanogens to conserve energy
286 to support growth from electron transport to extracellular electron acceptors is warranted.
287 Most methanogens, including other *Methanosarcina* species, lack membrane-bound
288 multi-heme cytochromes like MmcA and would need other mechanisms for extracellular
289 electron transfer. The finding that MmcA is not essential for methane production, and
290 that expression of *mmcA* was increased when AQDS served as an electron acceptor,
291 suggests that the primary role of MmcA is extracellular electron transfer. If so, the
292 presence of MmcA in *M. acetivorans* further suggests that there are environments in
293 which the capacity for extracellular electron transfer substantially benefits *M.*
294 *acetivorans*.

295 A wide diversity of archaea are capable of extracellular electron transfer (72), but
296 the mechanisms are poorly understood. For archaea such as *Ferroglobus placidus* (23),
297 *Geoglobus ahangari* (24), and diverse ANME (13-19) it has been proposed that outer-

298 membrane cytochromes are the terminal reductase. The rapid non-physiological reduction
299 of extracellular electron acceptors by a range of redox-active proteins and co-factors *in*
300 *vitro* necessitates genetically tractable model organisms for physiologically relevant
301 functional studies. Thus, *M. acetivorans* may serve as an important model organism for
302 better understanding cytochrome-based extracellular electron transfer in Archaea.

303 **Materials and Methods**

304 **Strains and growth conditions**

305 *Methanosarcina acetivorans* strains were routinely cultured under strict anaerobic
306 conditions at 37°C in the previously described (25) medium with either 8.5 mM methanol
307 or 40 mM acetate provided as substrates.

308 *M. acetivorans* mutant strains were constructed with *M. acetivorans* WWM1
309 (Δhpt) (73) as the parent strain as described previously (26). For construction of
310 MA0658, MA3739, MA2908, MA0167, and MA2925 deletion strains, genes were
311 replaced with the *pac* gene (puromycin resistance gene). First, regions 500-1000 bp
312 upstream and downstream from the target genes were amplified by PCR (Supplementary
313 Table S4). The DNA fragments of the upstream and downstream regions of MA0658
314 were digested with SacI/XbaI and EcoRI/XhoI. Upstream and downstream regions of
315 MA3739 were digested with Sall/XbaI and SacI/NotI. Upstream and downstream regions
316 of MA2908, MA0167, and MA2925 were digested with XhoI/HindIII and BamHI/NotI.
317 The upstream fragment was ligated into the pJK3 plasmid (25). The downstream
318 fragment was ligated into the pJK3 plasmid already containing the upstream fragment.
319 This recombinant plasmid was then linearized and used for transformation. The deletion
320 and replacement of all genes with *pac* was verified with primers (Supplementary Table

321 S4). All transformants were selected on medium supplemented with puromycin (2 μ M
322 final concentration), as previously described (25).

323 Additions of anthraquinone-2,6,-disulphonate (AQDS) were made from a
324 concentrated stock to provide a final concentration of 16 mM. Cysteine was omitted from
325 all cultures. When noted, 2-bromoethanesulfonate (BES) was added from a concentrated
326 stock to provide a final concentration of 15 mM. Growth with AQDS was measured by
327 determining numbers of cells stained with acridine orange with epifluorescence
328 microscopy (74). For comparing methanogenic growth in wild-type and mutant cells,
329 growth was monitored by spectrometry at an absorbance of 600 nm (75).

330 **Analytical techniques**

331 Methanol concentrations were monitored with a gas chromatograph equipped
332 with a headspace sampler and a flame ionization detector (Clarus 600; PerkinElmer Inc.,
333 CA). Methane in the headspace was measured by gas chromatography with a flame
334 ionization detector (Shimadzu, GC-8A) as previously described (76). Production of
335 reduced AQDS reduction was monitored by spectrophotometry at an absorbance of 450
336 nm as previously described (77).

337 **RNA extraction**

338 Cells were harvested from triplicate 50 mL cultures of *M. acetivorans* grown with
339 methanol (10 mM) provided as the electron donor and AQDS (16 mM) in the presence of
340 the methanogenesis inhibitor BES (15 mM) or via methanogenesis with 40 mM methanol
341 provided as substrate. Cells were split into 50 mL conical tubes (BD Sciences), mixed
342 with RNA Protect (Qiagen) in a 1:1 ratio, and pelleted by centrifugation at 3,000 x g for
343 15 minutes at 4°C. Pellets were then immediately frozen in liquid nitrogen and stored at -

344 80 °C. Total RNA was extracted from all six cell pellets according to the previously
345 described protocol (78) and cleaned with the RNeasy Mini Kit (Qiagen). All RNA
346 samples were then treated with Turbo DNA-free DNase (Ambion, Austin, TX). In order
347 to ensure that samples were not contaminated with genomic DNA, PCR with primers
348 targeting the 16S rRNA gene was done with RNA that had not been reverse transcribed.
349 Further enrichment of mRNA was done with the MICROBExpress kit (Ambion),
350 according to the manufacturer's instructions.

351

352 **RT-PCR analysis**

353 Total RNA was prepared from *M. acetivorans* hpt and Δ MA0658 strains grown
354 methanogenically with acetate (40 mM). Complementary DNA (cDNA) was prepared by
355 reverse transcription with AMV reverse transcriptase (New England Biolabs, MA) with
356 primers TCAGCATGCCTCATTCCAAC (MA0659) or
357 TCGCAGACAGCCTTAACGTC (MA0664) according to the manufacturers
358 specifications. This cDNA was then used as a template for PCR with the following
359 primer pairs: CAGTGACCTCGCTTATGTCC/TCAGCATGCCTCATTCCAAC
360 (MA0695) or TGTGGAGGTTGCGGATTTGC/TCGCAGACAGCCTTAACGTC
361 (MA0664). The amplified fragments were analyzed by agarose gel electrophoresis.

362

363 **Illumina sequencing and data analysis.**

364 Directional multiplex libraries were prepared with the ScriptSeq™ v2 RNA-Seq
365 Library Preparation Kit (Epicentre) and paired end sequencing was performed on a Hi-

366 Seq 2000 platform at the Deep Sequencing Core Facility at the University of
367 Massachusetts Medical School in Worcester, Massachusetts.

368 All raw data generated by Illumina sequencing were quality checked by
369 visualization of base quality scores and nucleotide distributions with FASTQC
370 (<http://www.bioinformatics.babraham.ac.uk/projects/fastqc/>). Initial raw non-filtered
371 forward and reverse sequencing libraries contained an average of 124,551,285 +/-
372 8,421,388 reads that were ~100 basepairs long. Sequences from all of the libraries were
373 trimmed and filtered with Trimmomatic (79) with the sliding window approach set to
374 trim bases with quality scores lower than 3, strings of 3+N's, and reads with a mean
375 quality score lower than 20. Bases were also cut from the start and end of reads that fell
376 below a threshold quality of 3, and any reads smaller than 50 bp were eliminated from the
377 library. These parameters yielded an average of 115,861,910 +/- 2,278,492 quality reads
378 per RNAseq library.

379 All paired-end reads were then merged with FLASH (80), resulting in 45,331,795
380 +/- 3,260,585 reads with an average read length of 145 basepairs. After merging the QC-
381 filtered reads, SortMeRNA (81) was used to separate all ribosomal RNA (rRNA) reads
382 from non-ribosomal reads.

383 **Mapping of mRNA reads**

384 Trimmed and filtered mRNA reads from the triplicate samples for the two
385 different culture conditions were mapped against the *M. acetivorans* strain C2A genome
386 (NC_003552) downloaded from IMG/MER (img.jgi.doe.gov). Mapped reads were
387 normalized with the RPKM (reads assigned per kilobase of target per million mapped
388 reads) method (82, 83) using ArrayStar software (DNASTar). Analysis of reads from all

389 three biological replicates for each condition demonstrated that results were highly
390 reproducible. Therefore, all reported values were obtained after merging and averaging
391 replicates. Expression levels were considered significant only when the \log_2 RPKM value
392 was higher than that of the median \log_2 RPKM. Out of the 4721 predicted protein-coding
393 genes in the *M. acetivorans* C2A genome, 2360 and 2362 had expression levels that were
394 higher than the median in AQDS-respiring or methanogenic cells, respectively
395 (Supplementary Table S1).

396 Reads were also normalized and processed for differential expression studies
397 using the edgeR package in Bioconductor (84). Genes with p-values ≤ 0.05 and fold
398 changes ≥ 2 were considered differentially expressed. Using these criteria, 827 genes
399 were up-regulated and 778 genes were down-regulated in AQDS-respiring cells
400 compared to methanogenic cells (Supplementary Table S5).

401 **Genome data analysis**

402 Gene sequence data for *M. acetivorans* C2A was acquired from the US
403 Department of Energy Joint Genome Institute (<http://www.jgi.doe.gov>) or from Genbank
404 at the National Center for Biotechnology Information (NCBI)
405 (<http://www.ncbi.nlm.nih.gov>). Initial analyses were done with tools available on the
406 Integrated Microbial Genomes (IMG) website (img.jgi.doe.gov). Some protein domains
407 were identified with NCBI conserved domain search (85) and Pfam search (86) functions.
408 Transmembrane helices were predicted with TMpred (87), TMHMM (88), and
409 HMMTOP (89) and signal peptides were identified with PSORTb v. 3.0.2 (90) and
410 Signal P v. 4.1 (91).

411

412 **Accession numbers**

413 Illumina sequence reads have been submitted to the NCBI database under
414 BioProject PRJNA501858 and submission number SUB4712594.

415

416 **Acknowledgments**

417 This research was supported by the Army Research Office and was accomplished under
418 Grant Number W911NF-17-1-0345. The views and conclusions contained in this
419 document are those of the authors and should not be interpreted as representing the
420 official policies, either expressed or implied, of the Army Research Office or the U.S.
421 Government.

422 **References**

- 423 1. Vargas M, Kashefi K, Blunt-Harris EL, Lovley DR. 1998. Microbiological evidence for
424 Fe(III) reduction on early Earth. *Nature* 395:65-67.
- 425 2. Bond DR, Lovley DR. 2002. Reduction of Fe(III) oxide by methanogens in the
426 presence and absence of extracellular quinones. *Environ Microbiol* 4:115-124.
- 427 3. Cervantes FJ, de Bok FAM, Tuan DD, Stams AJM, Lettinga G, Field JA. 2002. Reduction
428 of humic substances by halorespiring, sulphate-reducing and methanogenic
429 microorganisms. *Environ Microbiol* 4:51-57.
- 430 4. Bodegom PM, Scholten JC, Stams AJ. 2004. Direct inhibition of methanogenesis by
431 ferric iron. *FEMS Microbiol Ecol* 49:261-8.
- 432 5. Liu D, Dong HL, Bishop ME, Wang HM, Agrawal A, Tritschler S, Eberl DD, Xie SC.
433 2011. Reduction of structural Fe(III) in nontronite by methanogen *Methanosarcina*
434 *barkeri*. *Geochim Cosmochim Acta* 75:1057-1071.
- 435 6. Zhang J, Dong HL, Liu D, Fischer TB, Wang S, Huang LQ. 2012. Microbial reduction of
436 Fe(III) in illite-smectite minerals by methanogen *Methanosarcina mazei*. *Chem Geol*
437 292:35-44.
- 438 7. Zhang J, Dong HL, Zhao LD, McCarrick R, Agrawal A. 2014. Microbial reduction and
439 precipitation of vanadium by mesophilic and thermophilic methanogens. *Chem Geol*
440 370:29-39.
- 441 8. Sivan O, Shusta SS, Valentine DL. 2016. Methanogens rapidly transition from
442 methane production to iron reduction. *Geobiology* 14:190-203.
- 443 9. Holmes DE, Orelana R, Giloteaux L, Wang LY, Shrestha P, Williams K, Lovley DR,
444 Rotaru AE. 2018. Potential for methanosarcina to contribute to uranium reduction
445 during acetate-promoted groundwater bioremediation. *Microb Ecol* 76:660-667.
- 446 10. Rotaru AE, Shrestha PM, Liu F, Markovaita B, Chen S, Nevin KP, Lovley DR. 2014.
447 Direct interspecies electron transfer between *Geobacter metallireducens* and
448 *Methanosarcina barkeri*. *Appl Environ Microbiol* 80:4599-605.

- 449 11. Rotaru AE, Shrestha PM, Liu FH, Shrestha M, Shrestha D, Embree M, Zengler K,
450 Wardman C, Nevin KP, Lovley DR. 2014. A new model for electron flow during
451 anaerobic digestion: direct interspecies electron transfer to *Methanosaeta* for the
452 reduction of carbon dioxide to methane. *Energy Environ Sci* 7:408-415.
- 453 12. Holmes DE, Shrestha PM, Walker DJF, Dang Y, Nevin KP, Woodard TL, Lovley DR.
454 2017. Metatranscriptomic Evidence for Direct Interspecies Electron Transfer
455 between *Geobacter* and *Methanothrix* Species in Methanogenic Rice Paddy Soils.
456 *Appl Environ Microbiol* 83.
- 457 13. Myerdierks A, Kube M, Kostadinov I, Teeling H, Glockner FO, Reinhardt R, Amann R.
458 2010. Metagenome and mRNA expression analyses of anaerobic methanotrophic
459 archaea of the ANME-1 group. *Environ Microbiol* 12:422-439.
- 460 14. McGlynn SE, Chadwick GL, Kempes CP, Orphan VJ. 2015. Single cell activity reveals
461 direct electron transfer in methanotrophic consortia. *Nature* 526:531-U146.
- 462 15. Wegener G, Krukenberg V, Riedel D, Tegetmeyer HE, Boetius A. 2015. Intercellular
463 wiring enables electron transfer between methanotrophic archaea and bacteria.
464 *Nature* 526:587-590.
- 465 16. McGlynn SE. 2017. Energy metabolism during anaerobic methane oxidation in
466 ANME Archaea. *Microbes Environ* 32:5-13.
- 467 17. Timmers PHA, Welte CU, Koehorst JJ, Plugge CM, Jetten MSM, Stams AJM. 2017.
468 Reverse methanogenesis and respiration in methanotrophic archaea. *Archaea*
469 2017:1654237.
- 470 18. Cai C, Leu AO, Xie G-J, Guo J, Feng Y, Zhao J-X, Tyson GW, Yuan Z, Hu S. 2018. A
471 methanotrophic archaeon couples anaerobic oxidation of methane to Fe(III)
472 reduction. *ISME J* 12:1929-1939.
- 473 19. Krukenberg V, Riedel D, Gruber-Vodicka HR, Buttigieg PL, Tegetmeyer HE, Boetius
474 A, Wegener G. 2018. Gene expression and ultrastructure of meso- and thermophilic
475 methanotrophic consortia. *Environ Microbiol* 20:1651-1666.
- 476 20. Shi L, Dong H, Reguera G, Beyenal H, Lu A, Liu J, Yu H-Q, Fredrickson JK. 2016.
477 Extracellular electron transfer mechanisms between microorganisms and minerals.
478 *Nat Rev Microbiol* 14:651-662.
- 479 21. Ueki T, DiDonato LN, Lovley DR. 2017. Toward establishing minimum requirements
480 for extracellular electron transfer in *Geobacter sulfurreducens*. *FEMS Microbiol Lett*
481 364:fnx093.
- 482 22. Aklujkar M, Coppi MV, Leang C, Kim BC, Chavan MA, Perpetua LA, Giloteaux L, Liu A,
483 Holmes DE. 2013. Proteins involved in electron transfer to Fe(III) and Mn(IV) oxides
484 by *Geobacter sulfurreducens* and *Geobacter uraniireducens*. *Microbiol* 159:515-35.
- 485 23. Smith JA, Aklujkar M, Risso C, Leang C, Giloteaux L, Holmes DE. 2015. Mechanisms
486 involved in Fe(III) respiration by the hyperthermophilic archaeon *Ferroglobus*
487 *placidus*. *Appl Environ Microbiol* 81:2735-44.
- 488 24. Manzella MP, Holmes DE, Rocheleau JM, Chung A, Reguera G, Kashefi K. 2015. The
489 complete genome sequence and emendation of the hyperthermophilic, obligate
490 iron-reducing archaeon "*Geoglobus ahangari*" strain 234(T). *Stand Genomic Sci*
491 10:77.
- 492 25. Metcalf WW, Zhang JK, Apolinario E, Sowers KR, Wolfe RS. 1997. A genetic system
493 for Archaea of the genus *Methanosarcina*: liposome-mediated transformation and
494 construction of shuttle vectors. *Proc Natl Acad Sci U S A* 94:2626-31.
- 495 26. Buan N, Kulkarni G, Metcalf W. 2011. Genetic methods for methanosarcina species.
496 *Methods Enzymol* 494:23-42.
- 497 27. Nayak DD, Metcalf WW. 2017. Cas9-mediated genome editing in the methanogenic
498 archaeon *Methanosarcina acetivorans*. *Proc Natl Acad Sci U S A* 114:2976-2981.

- 499 28. Soo VWC, McAnulty MJ, Tripathi A, Zhu F, Zhang L, Hatzakis E, Smith PB, Agrawal S,
500 Nazem-Bokae H, Gopalakrishnan S, Salis HM, Ferry JG, Maranas CD, Patterson AD,
501 Wood TK. 2016. Reversing methanogenesis to capture methane for liquid biofuel
502 precursors. *Microb Cell Fact* 15:11.
- 503 29. Yan Z, Joshi P, Gorski CA, Ferry JG. 2018. A biochemical framework for anaerobic
504 oxidation of methane driven by Fe(III)-dependent respiration. *Nature Comm*
505 9:1642.
- 506 30. Coppi MV, O'Neil RA, Leang C, Kaufmann F, Methé BA, Nevin KP, Woodard TL, Liu A,
507 Lovley DR. 2007. Involvement of *Geobacter sulfurreducens* SfrAB in acetate
508 metabolism rather than intracellular Fe(III) reduction. *Microbiol* 153:3572-3585.
- 509 31. Kletzin A, Heimerl T, Flechsler J, van Niftrik L, Rachel R, Klingl A. 2015. Cytochromes
510 c in Archaea: distribution, maturation, cell architecture, and the special case of
511 *Ignicoccus hospitalis*. *Front Microbiol* 6.
- 512 32. Kim B-C, Leang C, Ding YR, Glaven RH, Coppi MV, Lovley DR. 2005. OmcF, a putative
513 c-Type monoheme outer membrane cytochrome required for the expression of
514 other outer membrane cytochrome in *Geobacter sulfurreducens*. *J Bacteriol*
515 187:4505-13.
- 516 33. Kim B-C, Postier BL, DiDonato RJ, Chaudhuri SK, Nevin KP, Lovley DR. 2008. Insights
517 into genes involved in electricity generation in *Geobacter sulfurreducens* via whole
518 genome microarray analysis of the OmcF-deficient mutant. *Bioelectrochem* 73:70-
519 75.
- 520 34. Li X, Jones LH, Pearson AR, Wilmot CM, Davidson VL. 2006. Mechanistic possibilities
521 in MauG-dependent tryptophan tryptophylquinone biosynthesis. *Biochem*
522 45:13276-83.
- 523 35. Pearson AR, Jones LH, Higgins L, Ashcroft AE, Wilmot CM, Davidson VL. 2003.
524 Understanding quinone cofactor biogenesis in methylamine dehydrogenase through
525 novel cofactor generation. *Biochem* 42:3224-30.
- 526 36. Wang Y, Graichen ME, Liu A, Pearson AR, Wilmot CM, Davidson VL. 2003. MauG, a
527 novel diheme protein required for tryptophan tryptophylquinone biogenesis.
528 *Biochem* 42:7318-25.
- 529 37. Hoffmann M, Seidel J, Einsle O. 2009. CcpA from *Geobacter sulfurreducens* is a basic
530 di-heme cytochrome c peroxidase. *J Mol Biol* 393:951-65.
- 531 38. Atack JM, Kelly DJ. 2007. Structure, mechanism and physiological roles of bacterial
532 cytochrome c peroxidases. *Adv Microb Physiol* 52:73-106.
- 533 39. Schlegel K, Welte C, Deppenmeier U, Muller V. 2012. Electron transport during
534 acetoclastic methanogenesis by *Methanosarcina acetivorans* involves a sodium-
535 translocating Rnf complex. *FEBS J* 279:4444-52.
- 536 40. Li Q, Li L, Rejtar T, Lessner DJ, Karger BL, Ferry JG. 2006. Electron transport in the
537 pathway of acetate conversion to methane in the marine archaeon *Methanosarcina*
538 *acetivorans*. *J Bacteriol* 188:702-10.
- 539 41. Voordeckers JW, Kim BC, Izallalen M, Lovley DR. 2010. Role of *Geobacter*
540 *sulfurreducens* outer surface c-type cytochromes in reduction of soil humic acid and
541 anthraquinone-2,6-disulfonate. *Appl Environ Microbio* 76:2371-2375.
- 542 42. Bose A, Pritchett MA, Rother M, Metcalf WW. 2006. Differential regulation of the
543 three methanol methyltransferase isozymes in *Methanosarcina acetivorans* C2A. *J*
544 *Bacteriol* 188:7274-83.
- 545 43. Galagan JE, Nusbaum C, Roy A, Endrizzi MG, Macdonald P, FitzHugh W, Calvo S,
546 Engels R, Smirnov S, Atnoor D, Brown A, Allen N, Naylor J, Stange-Thomann N,
547 DeArellano K, Johnson R, Linton L, McEwan P, McKernan K, Talamas J, Tirrell A, Ye
548 W, Zimmer A, Barber RD, Cann I, Graham DE, Grahame DA, Guss AM, Hedderich R,

- 549 Ingram-Smith C, Kuettner HC, Krzycki JA, Leigh JA, Li W, Liu J, Mukhopadhyay B,
550 Reeve JN, Smith K, Springer TA, Umayam LA, White O, White RH, Conway de Macario
551 E, Ferry JG, Jarrell KF, Jing H, Macario AJ, Paulsen I, Pritchett M, Sowers KR, et al.
552 2002. The genome of *M. acetivorans* reveals extensive metabolic and physiological
553 diversity. *Genome Res* 12:532-42.
- 554 44. Bose A, Pritchett MA, Metcalf WW. 2008. Genetic analysis of the methanol- and
555 methylamine-specific methyltransferase 2 genes of *Methanosarcina acetivorans* C2A.
556 *J Bacteriol* 190:4017-26.
- 557 45. Wang M, Tomb JF, Ferry JG. 2011. Electron transport in acetate-grown
558 *Methanosarcina acetivorans*. *BMC Microbiol* 11:165.
- 559 46. Kulkarni G, Kridelbaugh DM, Guss AM, Metcalf WW. 2009. Hydrogen is a preferred
560 intermediate in the energy-conserving electron transport chain of *Methanosarcina*
561 *barkeri*. *PNAS* 106:15915-15920.
- 562 47. Abken HJ, Deppenmeier U. 1997. Purification and properties of an F₄₂₀H₂
563 dehydrogenase from *Methanosarcina mazei* Go1. *FEMS Microbiol Lett* 154:231-237.
- 564 48. Baumer S, Ide T, Jacobi C, Johann A, Gottschalk G, Deppenmeier U. 2000. The F₄₂₀H₂
565 dehydrogenase from *Methanosarcina mazei* is a redox-driven proton pump closely
566 related to NADH dehydrogenases. *J Biol Chem* 275:17968-17973.
- 567 49. Welte C, Deppenmeier U. 2011. Re-evaluation of the function of the F-420
568 dehydrogenase in electron transport of *Methanosarcina mazei*. *FEBS J* 278:1277-
569 1287.
- 570 50. Welte C, Deppenmeier U. 2014. Bioenergetics and anaerobic respiratory chains of
571 acetoclastic methanogens. *Biochim Biophys Acta-Bioenergetics* 1837:1130-1147.
- 572 51. Suharti S, Wang M, de Vries S, Ferry JG. 2014. Characterization of the RnfB and RnfG
573 subunits of the Rnf complex from the archaeon *Methanosarcina acetivorans*. *PLoS*
574 *One* 9:e97966.
- 575 52. Ide T, Baumer S, Deppenmeier U. 1999. Energy conservation by the
576 H₂:heterodisulfide oxidoreductase from *Methanosarcina mazei* Go1: identification of
577 two proton-translocating segments. *J Bacteriol* 181:4076-80.
- 578 53. Heiden S, Hedderich R, Setzke E, Thauer RK. 1993. Purification of a cytochrome b
579 containing H₂:heterodisulfide oxidoreductase complex from membranes of
580 *Methanosarcina barkeri*. *Eur J Biochem* 213:529-35.
- 581 54. Heiden S, Hedderich R, Setzke E, Thauer RK. 1994. Purification of a 2 subunit
582 cytochrome-b containing heterodisulfide reductase from methanol grown
583 *Methanosarcina barkeri*. *Eur J Biochem* 221:855-861.
- 584 55. Hedderich R, Hamann N, Bennati M. 2005. Heterodisulfide reductase from
585 methanogenic archaea: a new catalytic role for an iron-sulfur cluster. *Biol Chem*
586 386:961-70.
- 587 56. Kumar VS, Ferry JG, Maranas CD. 2011. Metabolic reconstruction of the archaeon
588 methanogen *Methanosarcina acetivorans*. *BMC Syst Biol* 5:28.
- 589 57. Benedict MN, Gonnerman MC, Metcalf WW, Price ND. 2012. Genome-scale metabolic
590 reconstruction and hypothesis testing in the methanogenic archaeon
591 *Methanosarcina acetivorans* C2A. *J Bacteriol* 194:855-65.
- 592 58. Yoshikawa S, Shimada A. 2015. Reaction mechanism of cytochrome c oxidase. *Chem*
593 *Rev* 115:1936-89.
- 594 59. Morgado L, Dantas JM, Bruix M, Londer YY, Salgueiro CA. 2012. Fine tuning of redox
595 networks on multiheme cytochromes from *Geobacter sulfurreducens* drives
596 physiological electron/proton energy transduction. *Bioinorg Chem Appl*
597 2012:298739.

- 598 60. Louro RO, Catarino T, Turner DL, Picarra-Pereira MA, Pacheco I, LeGall J, Xavier AV.
599 1998. Functional and mechanistic studies of cytochrome c3 from *Desulfovibrio gigas*:
600 thermodynamics of a "proton thruster". *Biochem* 37:15808-15.
- 601 61. Morgado L, Bruix M, Pessanha M, Londer YY, Salgueiro CA. 2010. Thermodynamic
602 characterization of a triheme cytochrome family from *Geobacter sulfurreducens*
603 reveals mechanistic and functional diversity. *Biophys J* 99:293-301.
- 604 62. Gunner MR, Mao J, Song Y, Kim J. 2006. Factors influencing the energetics of electron
605 and proton transfers in proteins. What can be learned from calculations. *Biochim*
606 *Biophys Acta* 1757:942-68.
- 607 63. Dantas JM, Morgado L, Aklujkar M, Bruix M, Londer YY, Schiffer M, Pokkuluri PR,
608 Salgueiro CA. 2015. Rational engineering of *Geobacter sulfurreducens* electron
609 transfer components: a foundation for building improved *Geobacter*-based
610 bioelectrochemical technologies. *Front Microbiol* 6:752.
- 611 64. Schlegel K, Leone V, Faraldo-Gomez JD, Muller V. 2012. Promiscuous archaeal ATP
612 synthase concurrently coupled to Na⁺ and H⁺ translocation. *PNAS* 109:947-952.
- 613 65. Jasso-Chavez R, Diaz-Perez C, Rodriguez-Zavala JS, Ferry JG. 2017. Functional Role of
614 MrpA in the MrpABCDEFG Na⁺/H⁺ Antiporter Complex from the Archaeon
615 *Methanosarcina acetivorans*. *J Bacteriol* 199.
- 616 66. Klupfel L, Piepenbrock A, Kappler A, Sander M. 2014. Humic substances as fully
617 regenerable electron acceptors in recurrently anoxic environments. *Nat Geosci*
618 7:195-200.
- 619 67. Thamdrup B. 2000. Bacterial manganese and iron reduction in aquatic sediments.
620 *Adv Microb Ecol Vol 16* 16:41-84.
- 621 68. Lovley DR. 1991. Dissimilatory Fe(III) and Mn(IV) reduction. *Microbiol Rev* 55:259-
622 87.
- 623 69. Keller J, Weisenhorn P, Megonigal J. 2009. Humic acids as electron acceptors in
624 wetland decomposition. *Soil Biol Biochem* 41:1518-1522.
- 625 70. Roden EE, Wetzel RG. 2003. Competition between Fe(III)-reducing and
626 methanogenic bacteria for acetate in iron-rich freshwater sediments. *Microb Ecol*
627 45:252-258.
- 628 71. Lovley DR, Phillips EJP. 1987. Competitive mechanisms for inhibition of sulfate
629 reduction and methane production in the zone of ferric iron reduction in sediments
630 *Appl Environ Microbiol* 53:2636-2641.
- 631 72. Lovley DR, Holmes DE, Nevin KP. 2004. Dissimilatory Fe(III) and Mn(IV) reduction.
632 *Adv Microb Physiol* 49:219-86.
- 633 73. Pritchett MA, Zhang JK, Metcalf WW. 2004. Development of a markerless genetic
634 exchange method for *Methanosarcina acetivorans* C2A and its use in construction of
635 new genetic tools for methanogenic archaea. *Appl Environ Microbiol* 70:1425-33.
- 636 74. Lovley DR, Phillips EJ. 1988. Novel mode of microbial energy metabolism: organic
637 carbon oxidation coupled to dissimilatory reduction of iron or manganese. *Appl*
638 *Environ Microbiol* 54:1472-80.
- 639 75. Mouser PJ, Holmes DE, Perpetua LA, DiDonato R, Postier B, Liu A, Lovley DR. 2009.
640 Quantifying expression of *Geobacter spp.* oxidative stress genes in pure culture and
641 during *in situ* uranium bioremediation. *ISME J* 3:454-465.
- 642 76. Holmes DE, Giloteaux L, Orellana R, Williams KH, Robbins MJ, Lovley DR. 2014.
643 Methane production from protozoan endosymbionts following stimulation of
644 microbial metabolism within subsurface sediments. *Front Microbiol* 5.
- 645 77. Lovley DR, Coates JD, Blunt-Harris EL, Phillips EJP, Woodward JC. 1996. Humic
646 substances as electron acceptors for microbial respiration. *Nature* 382:445-448.

- 647 78. Holmes DE, Risso C, Smith JA, Lovley DR. 2012. Genome-scale analysis of anaerobic
648 benzoate and phenol metabolism in the hyperthermophilic archaeon *Ferroglobus*
649 *placidus*. ISME J 6:146-57.
- 650 79. Bolger AM, Lohse M, Usadel B. 2014. Trimmomatic: a flexible trimmer for Illumina
651 sequence data. Bioinformatics 30:2114-20.
- 652 80. Magoc T, Salzberg SL. 2011. FLASH: fast length adjustment of short reads to improve
653 genome assemblies. Bioinformatics 27:2957-63.
- 654 81. Kopylova E, Noe L, Touzet H. 2012. SortMeRNA: fast and accurate filtering of
655 ribosomal RNAs in metatranscriptomic data. Bioinformatics 28:3211-7.
- 656 82. Mortazavi A, Williams BA, McCue K, Schaeffer L, Wold B. 2008. Mapping and
657 quantifying mammalian transcriptomes by RNA-Seq. Nat Methods 5:621-8.
- 658 83. Klevebring D, Bjursell M, Emanuelsson O, Lundeberg J. 2010. In-Depth
659 Transcriptome Analysis Reveals Novel TARs and Prevalent Antisense Transcription
660 in Human Cell Lines. Plos One 5.
- 661 84. Robinson MD, McCarthy DJ, Smyth GK. 2010. edgeR: a Bioconductor package for
662 differential expression analysis of digital gene expression data. Bioinformatics
663 26:139-40.
- 664 85. Marchler-Bauer A, Derbyshire MK, Gonzales NR, Lu S, Chitsaz F, Geer LY, Geer RC, He
665 J, Gwadz M, Hurwitz DI, Lanczycki CJ, Lu F, Marchler GH, Song JS, Thanki N, Wang Z,
666 Yamashita RA, Zhang D, Zheng C, Bryant SH. 2015. CDD: NCBI's conserved domain
667 database. Nucleic Acids Res 43:D222-6.
- 668 86. Finn RD, Coggill P, Eberhardt RY, Eddy SR, Mistry J, Mitchell AL, Potter SC, Punta M,
669 Qureshi M, Sangrador-Vegas A, Salazar GA, Tate J, Bateman A. 2016. The Pfam
670 protein families database: towards a more sustainable future. Nucleic Acids Res
671 44:D279-85.
- 672 87. Hofmann K, Stoffel W. 1993. TMBASE- A database of membrane spanning protein
673 segments. Biol Chem Hoppe-Seyler 374:166.
- 674 88. Krogh A, Larsson B, von Heijne G, Sonnhammer EL. 2001. Predicting
675 transmembrane protein topology with a hidden Markov model: application to
676 complete genomes. J Mol Biol 305:567-80.
- 677 89. Tusnady GE, Simon I. 2001. The HMMTOP transmembrane topology prediction
678 server. Bioinformatics 17:849-50.
- 679 90. Yu NY, Wagner JR, Laird MR, Melli G, Rey S, Lo R, Dao P, Sahinalp SC, Ester M, Foster
680 LJ, Brinkman FS. 2010. PSORTb 3.0: improved protein subcellular localization
681 prediction with refined localization subcategories and predictive capabilities for all
682 prokaryotes. Bioinformatics 26:1608-15.
- 683 91. Petersen TN, Brunak S, von Heijne G, Nielsen H. 2011. SignalP 4.0: discriminating
684 signal peptides from transmembrane regions. Nat Methods 8:785-6.

685

686 **Figure legends**

687 Figure 1. Growth of *Methanosarcina acetivorans* with methanol provided as an electron
688 donor and AQDS as an electron acceptor in the presence or absence of BES. (A) Methane
689 and AHQDS concentrations generated by cultures grown without BES; (B) Methane and

690 AHQDS concentrations generated by cultures grown with BES; (C) Methanol
691 concentrations and (D) cell numbers from cultures grown in the presence or absence of
692 BES. The complete inhibition of methane production in the presence of BES is also
693 shown on an expanded scale in Supplementary Figure S1.

694 Figure 2. Impact of deletion of *c*-type cytochrome genes on growth of *M. acetivorans*
695 under different conditons. (A) AHQDS production during growth with methanol as the
696 electron donor and AQDS as the acceptor in the presence of BES. The locus ID for the
697 deleted cytochrome gene is designated next to the corresponding symbol. (B) Growth of
698 wild-type and Δ MA0658 strains under methanogenic conditions as measured by A_{600} with
699 methanol or acetate provided as substrates.

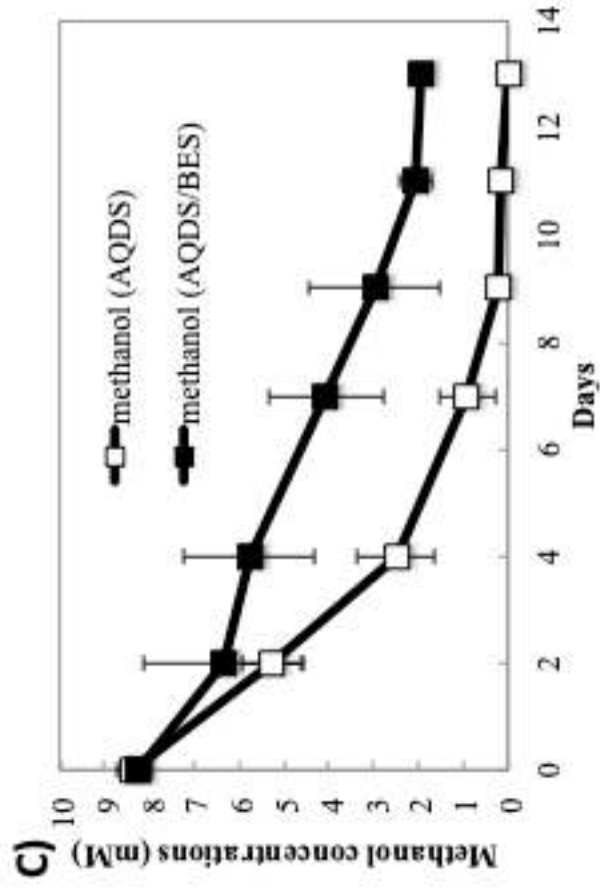
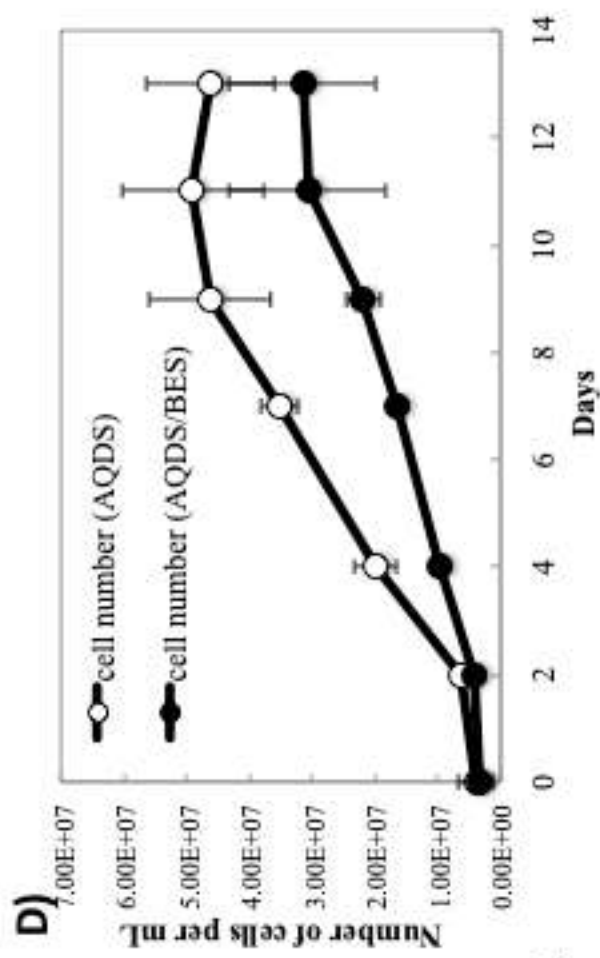
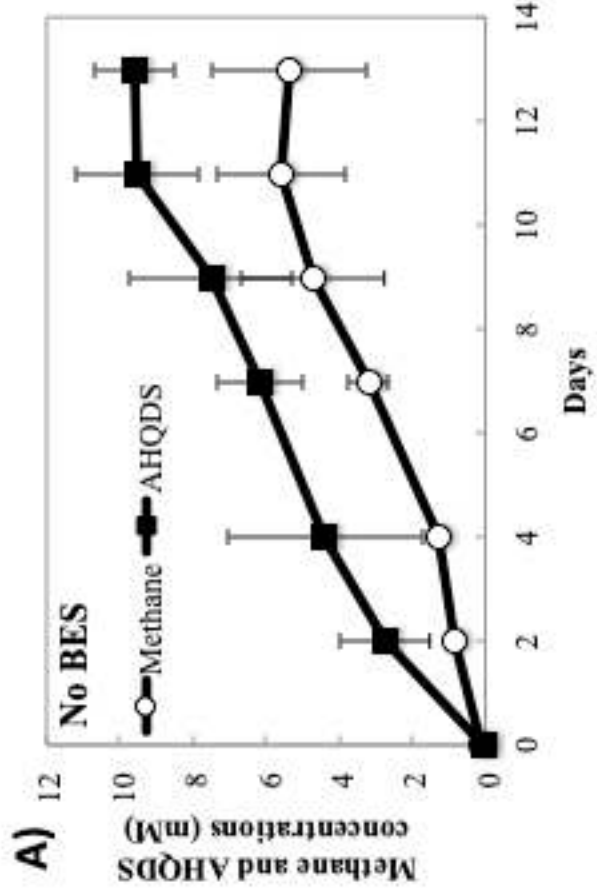
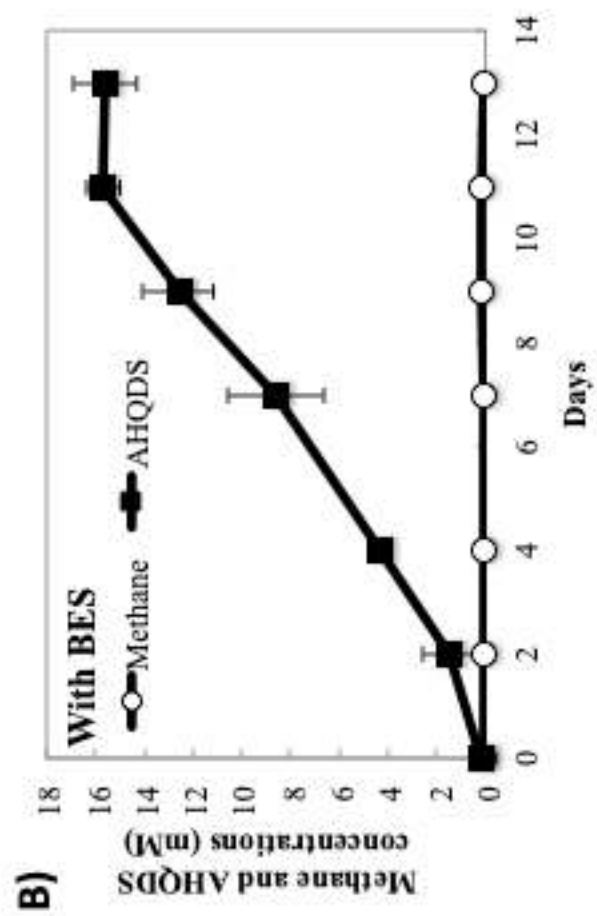
700 Figure 3. Proposed model for extracellular electron transport to AQDS by
701 *Methanosarcina acetivorans* when methanol is provided as the electron donor and
702 methanogenesis is prevented with the addition of BES.

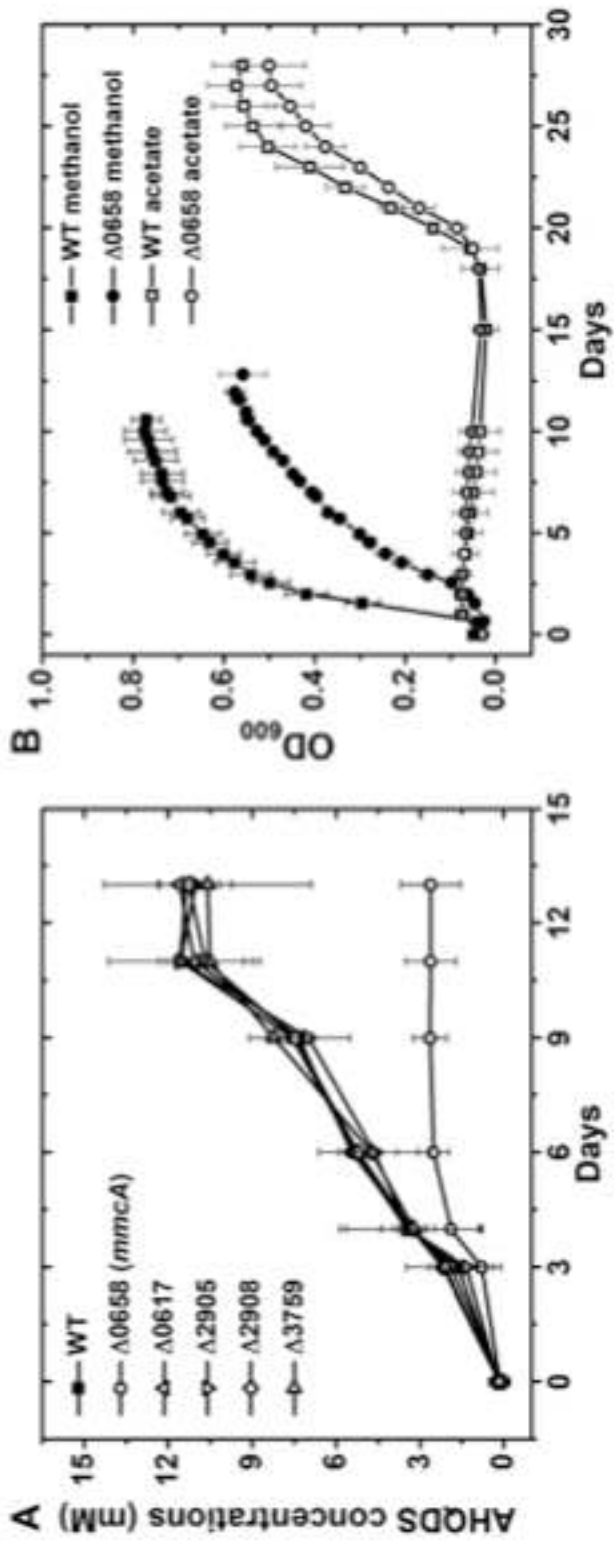
703

704

705

706





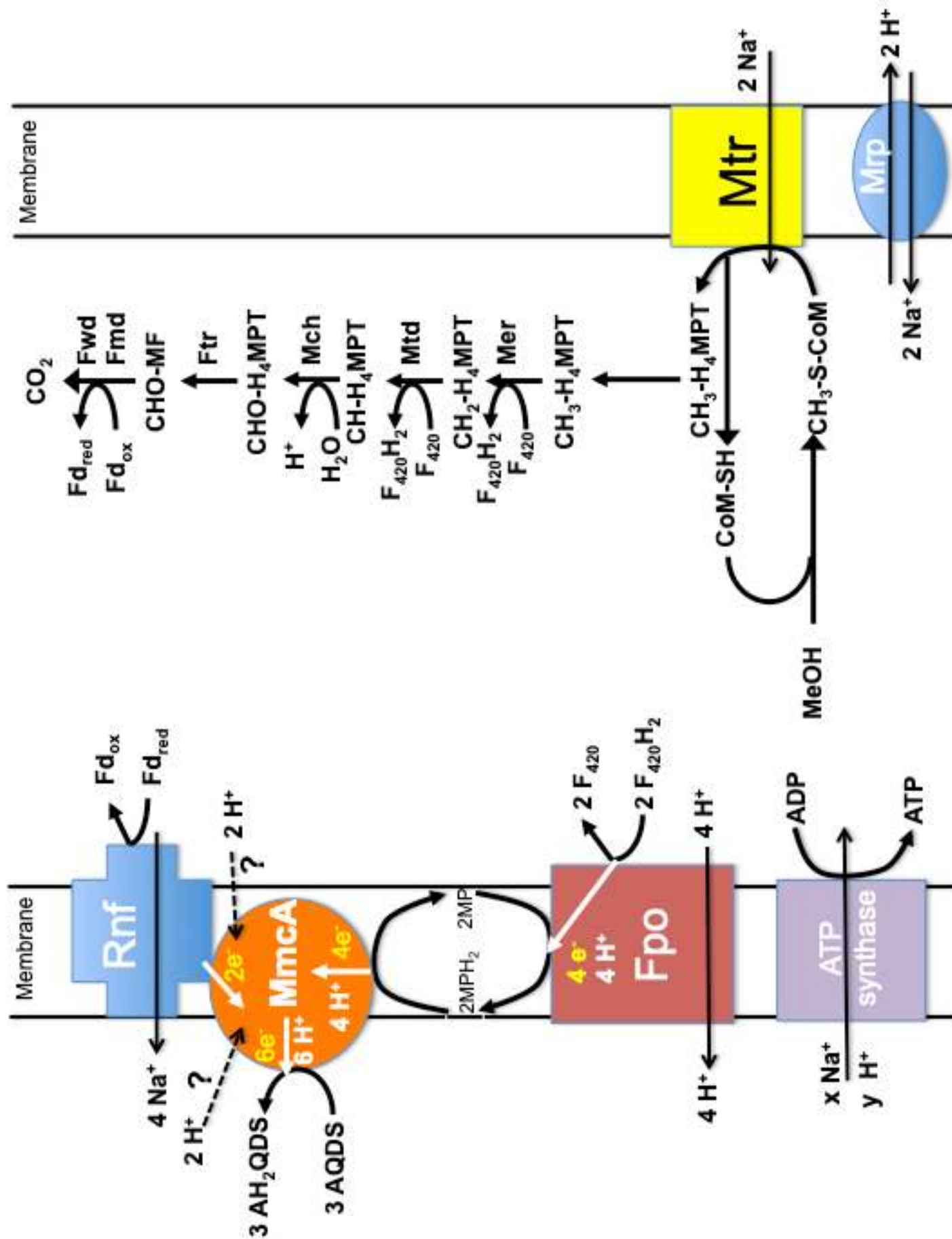


Table 1. Differential expression of genes coding for *c*-type cytochrome proteins in *M. acetivorans* cells grown with methanol provided as the electron donor and AQDS as the electron acceptor in the presence of BES, or cells grown via methanogenesis with methanol as the substrate. Genes were only considered differentially expressed if the fold change was ≥ 2 and the P-value and FDR (False Discovery Rate) were <0.05 .

NS: no significant difference in read abundance between conditions

| Locus ID | # heme groups | # transmembrane helices | Predicted Localization | Fold up-regulated in AQDS/BES vs methanogenesis | P-value | FDR |
|---------------|---------------|-------------------------|------------------------|---|---------|-------|
| MA0658 | 7 | 1 | Membrane | 3.95 | 0.002 | 0.006 |
| MA3739 | 5 | 0 | Unknown | 4.14 | 0.009 | 0.02 |
| MA0167 | 1 | 1 | Membrane | 5.97 | 0.002 | 0.006 |
| MA2925 | 2 | 1 | Membrane | 1.21 (NS) | 0.29 | 0.37 |
| MA2908 | 2 | 1 | Membrane | 1.03 (NS) | 0.87 | 0.89 |

Table 2. Comparison of transcripts from genes coding for components of the Rnf and Mrp complexes in *M. acetivorans* cells grown with methanol and AQDS in the presence of BES, or cells grown via methanogenesis with methanol. egative values indicate that genes were more significantly expressed in methanogenic cells. Genes were only considered differentially expressed if the fold change was ≥ 2 and the P-value and FDR (False Discovery Rate) were <0.05 . NS: no significant difference in read abundance

| Locus ID | Annotation | Gene | Fold up-regulated in AQDS/BES vs methanogenesis | P-value | FDR |
|----------|---|-------------|---|-----------------------|-----------------------|
| MA0659 | electron transport complex protein RnfC | <i>rnfC</i> | 1.52 (NS) | 0.02 | 0.04 |
| MA0660 | electron transport complex protein RnfD | <i>rnfD</i> | 1.23 (NS) | 0.19 | 0.26 |
| MA0661 | electron transport complex protein RnfG | <i>rnfG</i> | 1.66 (NS) | 0.006 | 0.01 |
| MA0662 | electron transport complex protein RnfE | <i>rnfE</i> | 1.45 (NS) | 0.02 | 0.05 |
| MA0663 | electron transport complex protein RnfA | <i>rnfA</i> | 1.66 (NS) | 0.006 | 0.01 |
| MA0664 | electron transport complex protein RnfB | <i>rnfB</i> | 1.57 (NS) | 0.008 | 0.01 |
| MA4572 | multisubunit sodium/proton antiporter, MrpA subunit | <i>mrpA</i> | 5.44 | 8.87×10^{-8} | 8.13×10^{-6} |
| MA4665 | multisubunit sodium/proton antiporter, MrpB subunit | <i>mrpB</i> | 5.41 | 1.57×10^{-7} | 1.07×10^{-5} |
| MA4570 | multisubunit sodium/proton antiporter, MrpC subunit | <i>mrpC</i> | 6.50 | 1.21×10^{-7} | 9.14×10^{-6} |
| MA4569 | multisubunit sodium/proton antiporter, MrpD subunit | <i>mrpD</i> | 4.84 | 2.05×10^{-7} | 1.18×10^{-5} |
| MA4568 | multisubunit sodium/proton antiporter, MrpE subunit | <i>mrpE</i> | 3.70 | 6.32×10^{-6} | 8.86×10^{-5} |
| MA4567 | multisubunit sodium/proton antiporter, MrpF subunit | <i>mrpF</i> | 4.79 | 5.21×10^{-7} | 1.86×10^{-5} |
| MA4566 | multisubunit sodium/proton antiporter, MrpG subunit | <i>mrpG</i> | 4.57 | 5.70×10^{-7} | 1.98×10^{-5} |

Table 3. Differential expression of genes coding for methanol methyltransferase enzymes in *M. acetivorans* cells grown with methanol provided as an electron donor and AQDS provided as an electron acceptor in the presence of BES or cells grown via methanogenesis with methanol. Negative values indicate that genes were more significantly expressed in methanogenic cells. Genes were only considered differentially expressed if the fold change was ≥ 2 and the P-value and FDR (False Discovery Rate) were <0.05 .

NS: no significant difference in read abundance

| Locus ID | Annotation | Gene | Fold up-regulated in AQDS/BES vs methanogenesis | P-value | FDR |
|----------|--|--------------|---|------------------------|-----------------------|
| MA4379 | Co-methyl-5-hydroxybenzimidazolylcobamide:2-mercapto-ethanesulphonic acid methyltransferase, isozyme 1 | <i>mtaA1</i> | -1.68 | 0.008 | 0.02 |
| MA0455 | methanol:5-hydroxybenzimidazolylcobamide methyltransferase, isozyme 1 | <i>mtaB1</i> | -6.84 | 0.002 | 0.007 |
| MA0456 | corrinoid-containing methyl-accepting protein, isozyme 1 | <i>mtaC1</i> | -7.95 | 0.001 | 0.005 |
| MA4392 | methanol:5-hydroxybenzimidazolylcobamide methyltransferase, isozyme 2 | <i>mtaB2</i> | 68.55 | 1.53×10^{-10} | 6.88×10^{-7} |
| MA4391 | corrinoid-containing methyl-accepting protein, isozyme 2 | <i>mtaC2</i> | 48.28 | 8.34×10^{-10} | 1.25×10^{-6} |
| MA1615 | Co-methyl-5-hydroxybenzimidazolylcobamide:2-mercapto-ethanesulphonic acid methyltransferase, isozyme 2 | <i>mtaA2</i> | 5.39 | 3.40×10^{-7} | 1.50×10^{-5} |
| MA1616 | methanol:5-hydroxybenzimidazolylcobamide methyltransferase, isozyme 3 | <i>mtaB3</i> | 9.66 | 7.45×10^{-8} | 7.56×10^{-6} |
| MA1617 | corrinoid-containing methyl-accepting protein, isozyme 3 | <i>mtaC3</i> | 8.49 | 3.78×10^{-7} | 1.55×10^{-5} |